

Diagnosis of multilayer clouds using photon path length distributions

Siwei Li¹ and Qilong Min¹

Received 28 December 2009; revised 5 June 2010; accepted 11 June 2010; published 19 October 2010.

[1] Photon path length distribution is sensitive to 3-D cloud structures. A detection method for multilayer clouds has been developed, by utilizing the information of photon path length distribution. The photon path length method estimates photon path length information from the low level, single-layer cloud structure that can be accurately observed by a millimeter-wave cloud radar (MMCR) combined with a micropulse lidar (MPL). As multiple scattering within the cloud layers and between layers would substantially enhance the photon path length, the multilayer clouds can be diagnosed by evaluating the estimated photon path information against observed photon path length information from a co-located rotating shadowband spectrometer (RSS). The measurements of MMCR-MPL and RSS at the Atmospheric Radiation Measurement (ARM) Southern Great Plains (SGP) site have been processed for the year 2000. Cases studies illustrate the consistency between MMCR-MPL detection and the photon path length method under most conditions. However, the photon path length method detected some multilayer clouds that were classified by the MMCR-MPL as single-layer clouds. From 1 year statistics at the ARM SGP site, about 27.7% of single-layer clouds detected by the MMCR-MPL with solar zenith angle less than 70° and optical depth greater than 10 could be multilayer clouds. It suggests that a substantial portion of single-layer clouds detected by the MMCR-MPL could also be influenced by some “missed” clouds or by the 3-D effects of clouds.

Citation: Li, S., and Q. Min (2010), Diagnosis of multilayer clouds using photon path length distributions, *J. Geophys. Res.*, 115, D20202, doi:10.1029/2009JD013774.

1. Introduction

[2] Detailed knowledge of the radiative properties of atmospheric constituents is crucial to properly characterize climate forcing mechanisms and quantify the response of the climate system. An important challenge is detecting the three-dimensional (3-D) structure of clouds and aerosols, and properly modeling the effects of this structure on radiative transfer. This is essential to reduce ambiguity in the retrieval of atmospheric properties and to improve radiative parameterization in models. Current ability to resolve 3-D cloud structure is limited to scanning pulsed active sensors and imaging instruments. However, no single ground-based sensor has proven to be capable of doing the job for all of the wide variety of atmospheric cloud situations. In general, the laser devices are excellent for detecting essentially all clouds that are visible from the ground and are within the instruments' height range. The laser systems are unable to provide any information about higher cloud layers when lower liquid-water layers are present. The great strength of

radar is its ability to penetrate clouds and reveal multiple layers aloft. Although its sensitivity is impressive, the millimeter-wave cloud radar fails to detect some of these clouds, especially if the clouds are composed of small hydrometeors, or the clouds may be thinner than the radar sample volume depth resulting in partial beam filling and reduced reflectivity [*Clothetaux et al.*, 2000].

[3] Information of “missed” cloud layer is extremely important for the Broadband Heating Rate Profile (BBHRP), since “missed” upper layer clouds would substantially impact radiation heating profiles. Figure 1 shows the calculated shortwave (SW), longwave (LW), and total heating rates for a single-layer cloud, a double-layer water cloud, and an ice cloud over water cloud at solar zenith angle of 45°. For the LW calculation, we used the U.S. standard atmospheric profile. In the calculation of double-layer cloud cases, we added a “missed” water or ice cloud layer with water path of 10 g/m² (cloud optical depth about 1) above the lower water cloud layer and reduced the lower layer water cloud path to 190 g/m² to ensure the same total water path of 200 g/m² for all cases. The SW reaching the surface for three cases are 124.1, 122.8, and 122.5 w/m², respectively, whereas the upwelling SW at the top of the atmosphere (TOA) are 376.1, 377.5, and 379.5 w/m², respectively. Clearly, the differences of SW at both boundaries

¹Atmospheric Sciences Research Center, State University of New York at Albany, Albany, New York, USA.

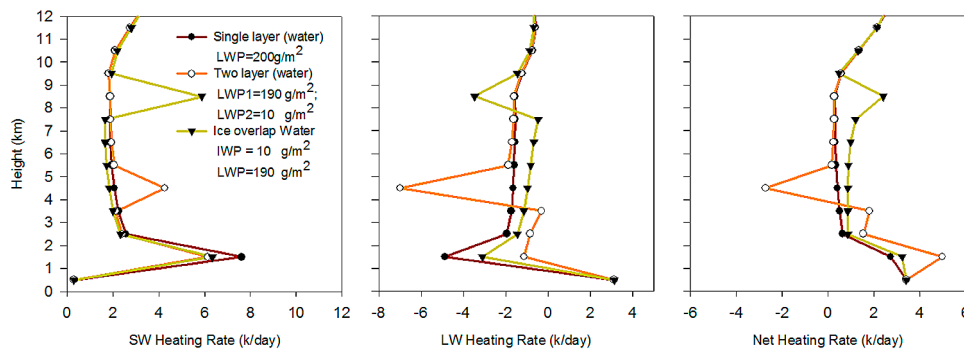


Figure 1. Broadband heating rate profile. IWP = Ice water path, LWP = Liquid water path.

with/without “missed” cloud layer are very small, within the measurement uncertainty. However, the heating rate profiles are substantially different. Although a “missed” cloud layer does not occur all the time, statistical information of “missed” cloud layer is extremely valuable for BBHRP. Furthermore, this simple calculation reinforces that the radiation closure at the boundaries cannot ensure the accuracy of the heating profile. There is an urgent need to exploit other means to detect the 3-D structure of clouds and aerosols.

[4] For a long time, the remote sensing community has recognized the advantages of using the oxygen A band and has sought ways to exploit these advantages to measure atmospheric properties and constituents. Because oxygen is a well-mixed gas in the atmosphere, the pressure dependence (as a surrogate of altitude) of oxygen A band absorption line parameters provides a vehicle for retrieving photon path length distributions from spectrometry of the oxygen A band. The concept underlying oxygen A band retrievals is the principle of equivalence, which allows assessment of atmospheric radiative properties at any nearby wavelength from a photon path length distribution measurement at one particular band [Irvine, 1964; 1966; van de Hulst, 1980]. This is possible because the scattering properties of cloud and aerosol vary slowly and predictably with wavelength and 760 nm is a useful central wavelength, reasonably representative of the entire solar shortwave. Photon path length distributions, a hidden property of standard radiation transfer models, are controlled by spatial distributions of scattering and absorption.

[5] Many efforts have been made to utilize photon path length distribution in oxygen A band as a tool in remote sensing [Grechko et al., 1973; Fischer and Grassl, 1991; Fischer et al., 1991; O’Brian and Mitchell, 1992; Harrison and Min, 1997; Pfeilsticker et al., 1998; Veitel et al., 1998; Min and Harrison, 1999; Portmann et al., 2001; Min et al., 2001; Min and Clothiaux, 2003; and Min et al., 2004; Min and Harrison, 2004; and many others]. In particular, Min and Clothiaux [2003] demonstrated that two independent pieces of information (mean and variance) are retrievable from a modest resolution Rotating Shadowband Spectrometer (RSS). Analysis of the variance and mean of the photon path length distribution from RSS measurements at the Atmospheric Radiation Measurement (ARM) Southern Great Plains (SGP) site illustrates how sensitive the photon path length distribution is to the cloud vertical profile. In this

study, we further exploit the unique potential of photon path length distribution to detect the 3-D structure of clouds and investigate how many clouds may be “missed” by the combination of a millimeter-wave cloud radar (MMCR) and a micropulse lidar (MPL) in a 1 year routine observation. Simply flagging possible “missed” clouds in routine MMCR-MPL observation is extremely valuable, as most ARM cloud products primarily use cloud retrievals from the MMCR.

2. Methodology

2.1. Retrieval of Oxygen A Band Photon Path Length Distribution

[6] On the basis of the equivalent theory, the relationship between radiances measured in a spectral region free of the molecular absorption (such as at wavelengths outside the oxygen A band) to radiances measured within an absorption line can be written as

$$I_\nu = I_0 \int_0^\infty p(l) e^{-k_\nu l} dl, \quad (1)$$

where I_0 and I_ν are radiances outside and within an absorption line, respectively, and $p(l)$ is the photon path length distribution. The transmission function $e^{-k_\nu l}$ depends on the optical path length l and gaseous absorption k_ν . The well-known effect of pressure broadening on line shape, which is a consequence of the dependency of k_ν on pressure P and temperature T reveals information about the distribution of photon path length with pressure. The photon path length distribution can be derived from an inverse Laplace transform. Min and Clothiaux [2003] have developed an approach to infer photon path length distributions from RSS measurements. This retrieval algorithm obtains empirical calibration coefficients of slit functions from clear-sky direct beam observations and applies them to diffuse irradiance measurements under cloudy sky conditions. Assuming $p(l)$ to be a simple γ distribution and using the existence of the Laplace transform, the photon path length distribution is retrieved from diffuse irradiance measurements. The detailed retrieval algorithm was provided by Min and Clothiaux [2003]. More important, on the basis of the information content analysis and RSS performance, Min and Clothiaux [2003] also provided the assessment of uncertainty in both mean and variance estimations from RSS

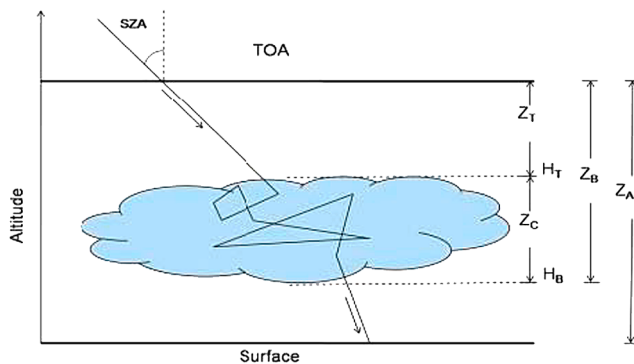


Figure 2. Schematic of photon path length in the atmosphere. H_T and H_B are the cloud top and base heights, respectively. Z_A , Z_T , and Z_B are the pressure-weighted oxygen cumulated paths for entire atmosphere, from the top of the atmosphere (TOA) to the cloud top, and from TOA to the cloud base, respectively. Z_C is the cumulated oxygen path of the cloud layer ($Z_C = Z_B - Z_T$).

measurements. We will apply the same algorithm for one-year data at the ARM SGP site.

2.2. Detection Method

[7] In a single-layer dense cloud with fixed physical depth, the photon path length scales linearly with optical depth, illustrating characteristics of classic Brownian diffusion with Gaussian statistics [Min *et al.*, 2001]. For a multilayered or complex cloud, a simple linear scaling does not exist. In the frame of photon diffusion theory, Davis and Marshak [2002] derived a mean-variance relation for a homogeneous media. As shown in the study by Min *et al.* [2004], the mean-variance curve with respect to a homogeneous model prediction provides a lower envelope on the observed data. It demonstrated the bias of 1-D theoretical calculation with respect to the more complicated 3-D observation. Such characteristics, therefore, provide a diagnostic tool of 3-D scattering and absorption structures in complex cloud systems. Our objective is to detect possible “missed” clouds, i.e., to flag possible multilayer or complex clouds that are detected by MMCR-MPL as single-layer clouds. Therefore, our detection strategy is (1) to estimate photon path information from the observed single-layer cloud structure of MMCR-MPL and optical properties retrieved from the Multifilter Rotating Shadowband Radiometer (MFRSR), based on 1-D diffusion theory; and (2) to detect the “missed” clouds by evaluating the estimated photon path information against observed photon path length information from a co-located RSS.

[8] For a single-layer cloud, sketched in Figure 2, the photon path length can be separated into three intrinsically linked parts: (1) transmitting from the top of the atmosphere to the cloud top, (2) scattering through the cloud layer, and (3) bouncing between the cloud base and the surface. The cloud geometry, i.e., the cloud top height (H_T) and the cloud base height (H_B) are determined by MMCR-MPL, whereas cloud optical depth is inferred from measurements from the MFRSR [Min and Harrison, 1996]. Since the photon path length observed through oxygen A band measurement is a pressure-weighted oxygen cumulated path length, we defined

the atmosphere and cloud geometry in terms of pressure-weighted oxygen cumulated path length, i.e., Z_A , Z_B , Z_C , and Z_T in Figure 2.

[9] To derive a simple baseline model for mean path length in the atmosphere, we parameterized each portion as follows:

[10] 1. Since there is not much scattering occurring above the cloud layer, the path length from the top of the atmosphere to the cloud top is simply, $M_T = Z_T/\cos(\text{SZA})$, where SZA is the solar zenith angle.

[11] 2. In the diffusion limit of multiple scattering, the mean path length (pressure-weighted oxygen mean path length) within the cloud layer is proportional to the product of cloud thickness Z_C (pressure-weighted oxygen cumulated path length in cloud) and vertical cloud optical depth τ , since the total number of scatterings for transmitted photons N is proportional to τ^2 and the total path length $M = \text{mfp}N = (H/\tau)\tau^2 = H\tau$ [Davis and Marshak, 2002]. Because of the photon penetration for the first scattering, the first scattering path length is sensitive to the location of the cloud top (Z_T is pressure-weighted oxygen cumulated path length from the top of cloud to the top of atmosphere) and solar zenith angle. Therefore, the total mean path length within the cloud layer can be expressed as $M_C = Z_C(c_1 + c_2\tau + c_3Z_T/(Z_A * \cos(\text{SZA})))$.

[12] 3. The mean path length due to the bounce between the cloud base and the surface can be assumed as $M_B = (Z_A - Z_B)\tau^{c_4}$, as cloud reflection is related to cloud optical depth.

[13] Therefore, the mean path length in the atmosphere for a single-layer cloud can be parameterized as

$$M = M_T + M_C + M_B = Z_T/\cos(\text{SZA}) + Z_C(c_1 + c_2\tau + c_3Z_T/(Z_A * \cos(\text{SZA}))) + (Z_A - Z_B)\tau^{c_4}.$$

The variance of photon path length is proportion to the square of the product of cloud geometric thickness and optical depth in diffusion limit [Davis and Marshak, 2002]. Similar to the mean path length, a simple model for variance is also developed as $\text{var} = p_1/\cos(\text{SZA})^2 + p_3Z_C^2\tau^2 + (Z_A - Z_B)^2\tau^{p_4}$, where c_1 , c_2 , c_3 , c_4 , p_1 , p_2 , p_3 , and p_4 are coefficients to be determined in the real atmosphere. To evaluate this parameterization and determine those coefficients, we used a Monte Carlo radiative transfer model to simulate thousands of cloud fields and associated photon path length distributions, including single-layer and multilayer clouds with various cloud locations, cloud thicknesses, and cloud optical depths. For single-layer clouds, we set cloud optical depth varying from 10 to 80, cloud base from 0 to 8 km, cloud thickness from 0.5 to 6 km, and solar zenith angle from 0° to 70° . For multilayer clouds, we added additional cloud layers above previous simulated single-layer clouds with different cloud properties. Although thousands of cloud fields may not include all possible cloud scenarios in the real atmosphere, they provide a basic set for understanding the relationship between photon path length information and cloud physical and optical properties, in terms of differentiating single-layer clouds from multilayer clouds.

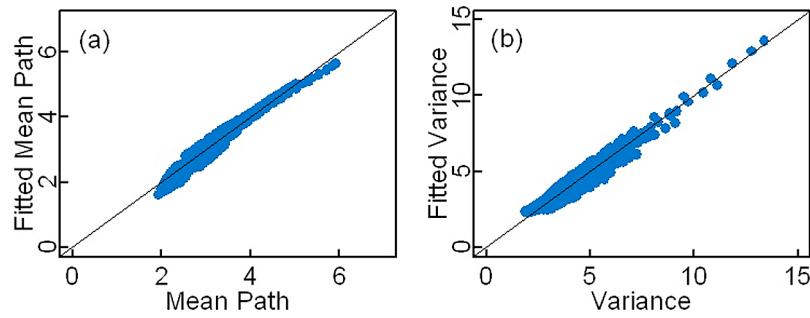


Figure 3. Fitted mean and variance compared to Monte Carlo radiative model-simulated mean and variance.

[14] The above simple parameterizations provide estimations of mean and variance of photon path length distribution for single-layer clouds, using the cloud geometric and optical properties observed from MMCR-MPL and MFRSR. Figure 3 shows the comparison of simulated and fitted mean and variance of photon path length distribution based on Monte Carlo simulations of single-layer clouds. The maximum differences between the simulated and fitted mean and variance are 0.5 and 1.3, respectively. Those maximum fitting errors provide detection limits for our method. For multilayer cloud systems, multiple scattering within the layers and between layers will substantially enhance the photon path length. If the observed mean path length (and/or variance) is much larger than the fitted mean (and/or fitted variance), i.e., greater than the maximum fitting errors, we flag it as a possible multilayer cloud. Specifically, as shown in Figure 4, all the single-layer clouds are located in the corner of the joint statistics of the Δ -mean (or the mean path length difference defined as observed (or “simulated”) mean – fitting mean) and the Δ -variance (or variance difference defined as observed (or “simulated”) variance – fitted variance), which distinctly separate them from most multilayer clouds (Figure 4b). Certainly, there are some multilayer clouds with the joint statistical characteristics overlapped with single-layer clouds. Those multilayer clouds may either have too small vertical separation between the layers or have the same first two moments as single-layer clouds with different higher moments of photon path length distribution. To further distinguish those multilayer clouds from single layer clouds, it requires higher resolution of

oxygen A band measurements that are able to retrieve higher moments of photon path length distribution. Given current resolution of RSS, only the first two moments can be retrieved [Min and Clothiaux, 2003]. Therefore, there are two possible thresholds for distinguishing multilayer clouds from single-layer clouds. The dashed line represents the normal thresholds, under which all single-layer clouds are included. It is determined by the maximum differences between the simulated and fitted mean and variance. Within this threshold, however, some multilayer clouds are treated as single-layer clouds. The black solid lines represent the conservative threshold, the values of which are 20% larger than the normal threshold on Δ -mean and 50% larger than the normal threshold on Δ -variance. The additional 20% and 50% in mean and variance are much more than the maximum fitting errors. Although this conservative threshold results in more multilayer clouds being identified as single-layer clouds, it provides the most conservative detection of possible “missed” clouds from MMCR-MPL single-layer clouds. As the diffusion theory holds for optically thick clouds, only clouds with optical depth greater than 10 will be considered in the observation.

3. Results

[15] We processed the measurements of MMCR, RSS, and MFRSR at the ARM SGP site for the year 2000. The cloud boundary and layer information were based on the Active Remotely Sensed Clouds Locations (ARSCL) that combined the measurements of MMCR and MPL [Clothiaux *et al.*, 2000]. The first two moments of photon path length

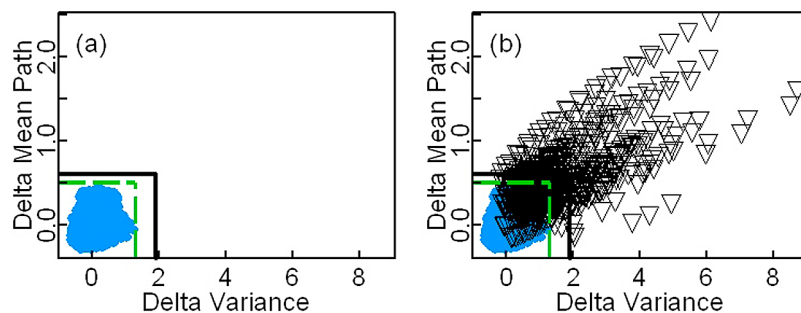


Figure 4. Δ -Mean and Δ -variance for single-layer cloud and multilayer cloud: (a) single-layer clouds (blue dots); (b) single-layer clouds (blue dots) and multilayer clouds (black triangles). The dashed green lines and solid black lines are for the normal threshold and the conservative threshold, respectively.

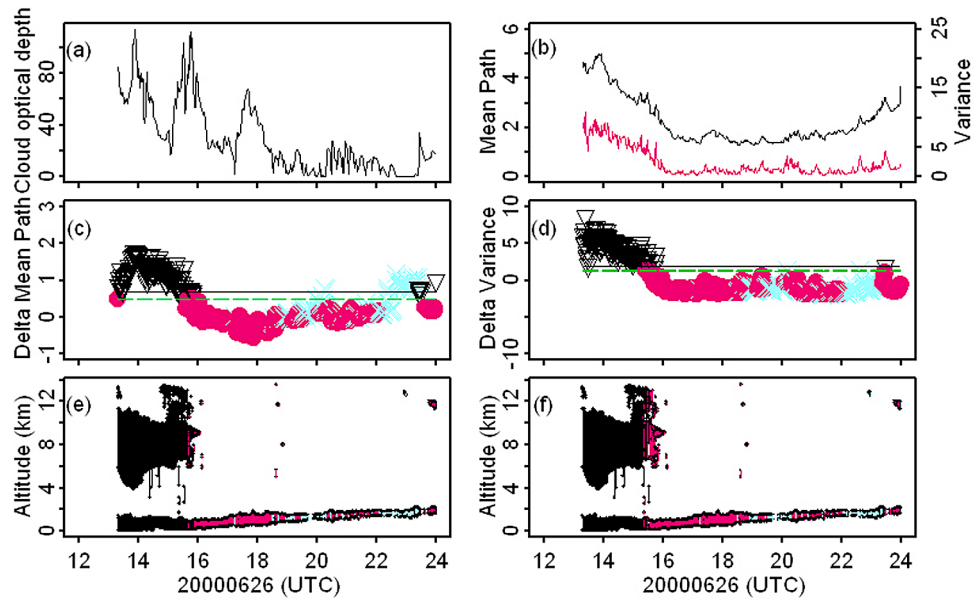


Figure 5. Time series plots. (a) Cloud optical depth retrieved from MFRSR; (b) mean path length (black line) and variance (red line) retrieved from RSS; (c) Δ -mean: the green dashed lines and black solid lines are for the normal and conservative thresholds, respectively; black triangles stand for those points over the normal threshold; (d) Δ -variance; (e) cloud profiles retrieved from MMCR-MPL with the combined normal threshold classification: black, red, and light blue colors stand for multilayer clouds, single-layer clouds, and optically thin clouds ($\tau > 10$), respectively; and (f) cloud profile classification with the combined conservative threshold.

distribution were retrieved from the RSS, whereas the cloud optical depth was obtained from the MFRSR. Before presenting year-long statistics, we showed four cases to illustrate the feasibility of our detection method.

3.1. Case 1 (26 June 2000)

[16] As shown in Figure 5e, on 26 June 2000, the MMCR-MPL detected a low-level cloud persistently through the day with multilayer clouds in the morning and late in the afternoon. Retrieved cloud optical depths from the MFRSR, shown in Figure 5a, varied from very thick (over 105) in the morning to very thin (less than 5) in the afternoon. Both inferred mean path length and variance from the RSS varied in concert with cloud optical depths (Figure 5b), which is consistent with our previous findings [Min *et al.*, 2001; Min and Clothiaux, 2003]. Substantial changes in solar zenith angle or air mass cause the both mean and variance of photon path length distribution to vary in a large range. Enhancements in both the mean and variance of photon path length distribution due to multilayer clouds are relatively smaller than the changes associated with variation of solar zenith angle. Therefore, the detection power of multilayer clouds directly from the mean and variance of photon path length distribution is limited.

[17] After properly removing the path length contribution from the lower layer clouds as outlined in section 2, the Δ -mean and Δ -variance, shown in Figures 5c and 5d, exhibit strong distinguishing power. On the basis of the normal (dashed line) or conservative (solid line) detection thresholds, cloud fields can be divided into multilayer clouds (black) and single-layer clouds (red), shown in Figures 5e

and 5f, respectively. Because of the limit of the diffusion theory, optically thin clouds (optical depth < 10) are excluded from analysis and marked as light blue. Clearly, most multilayer clouds observed by MMCR-MPL were identified by the photon path length method. Some multilayer clouds with a very thin upper layer were classified as being single layered by both thresholds. With the conservative threshold, more multilayer clouds were classified as single-layer clouds, as expected. This case illustrates the detection power of the photon path length method.

3.2. Case 2 (2 June 2000)

[18] The case of 2 June 2000, shown in Figure 6, was a special case where occasionally upper-level clouds appeared above a physically thick lower-level cloud deck. Because of the large thickness of the lower-level cloud, most of the photon path length was accumulated within the lower-level cloud layer. With the normal detection threshold, the Δ -mean diagnosed that this cloud system was a single-layer cloud. Even with the conservative detection threshold, the Δ -mean indicated that most clouds were single-layer clouds, except for some multilayer clouds around 19:00 UTC. It suggests that enhanced path length due to the upper layer cloud was relatively small and Δ -mean is not sensitive enough for this thick low level cloud situation. However, as shown in Figure 6d, the multilayer clouds diagnosed by Δ -variance were consistent with MMCR-MPL observation (Figures 6e–6f). The difference between the normal and conservative thresholds was small. It is clear that for thick low level cloud situation, Δ -variance is more sensitive to multilayer clouds than Δ -mean.

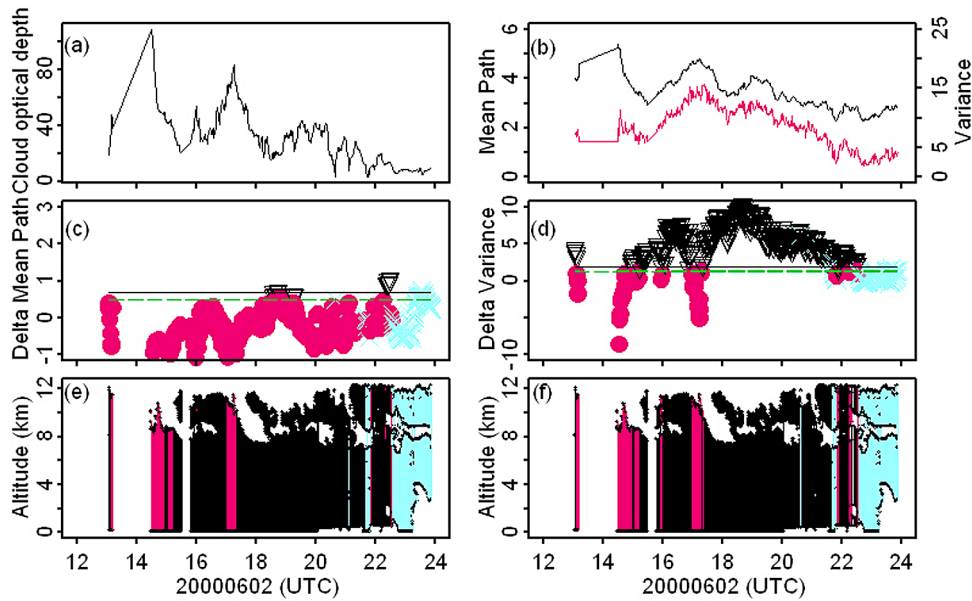


Figure 6. The same as Figure 5, but for 2 June 2000.

3.3. Case 3 (21 March 2000)

[19] Our photon path detection method based on diffusion theory is particularly good for optically thick situations. Clouds that occurred on 21 March 2000, as shown in Figure 7, were optically thick ($\tau > 30$). However, as the upper-level clouds were relatively thin compared to the lower-level clouds, our path length methods (Δ -mean and Δ -variance) classified some MMCR-MPL detected multilayer clouds as the single-layer cloud. It suggests that our detection of single-layer clouds is quite relaxed, allowing some interference of upper-level clouds. Keeping the relaxation in mind, it is interesting to see the period from 14.8 UTC and 15.7 UTC. During this

period, the MMCR-MPL detected just a single low-level cloud. However, both Δ -mean and Δ -variance with the conservative thresholds diagnosed this period as a multilayer cloud period. It means that under optically thick conditions, the radiation field, as indicated by photon path length distribution, violated the diffusion theory of a single-layer cloud. In other words, the radiation field was influenced by some clouds other than the MMCR-MPL-detected clouds. Those clouds were either out of the field of view of the MMCR-MPL but within the scale of cloud-radiation interaction or above the MMCR-MPL but having hydrometeors that were too small to be detected by the MMCR-MPL.

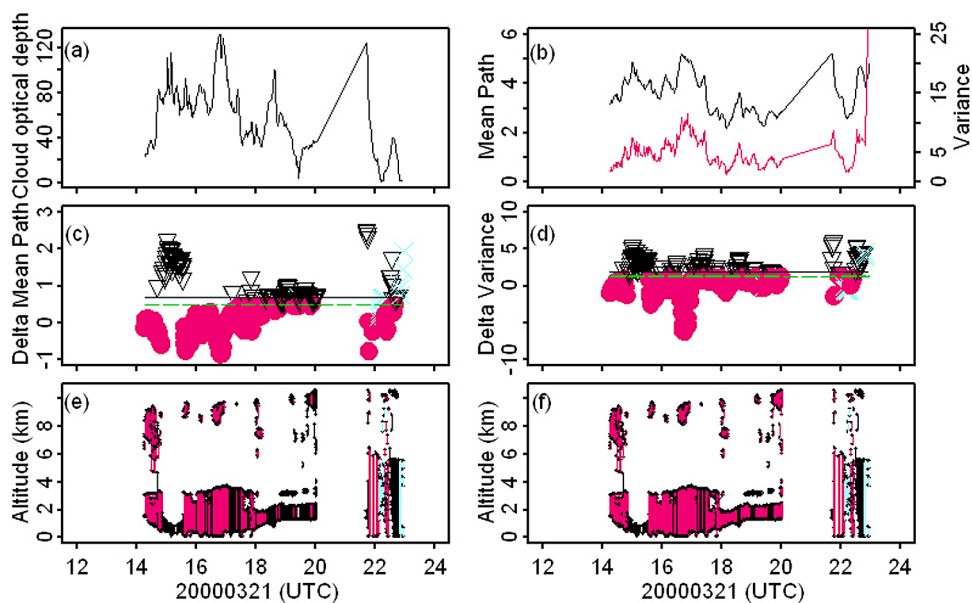


Figure 7. The same as Figure 5, but for 21 March 2000.

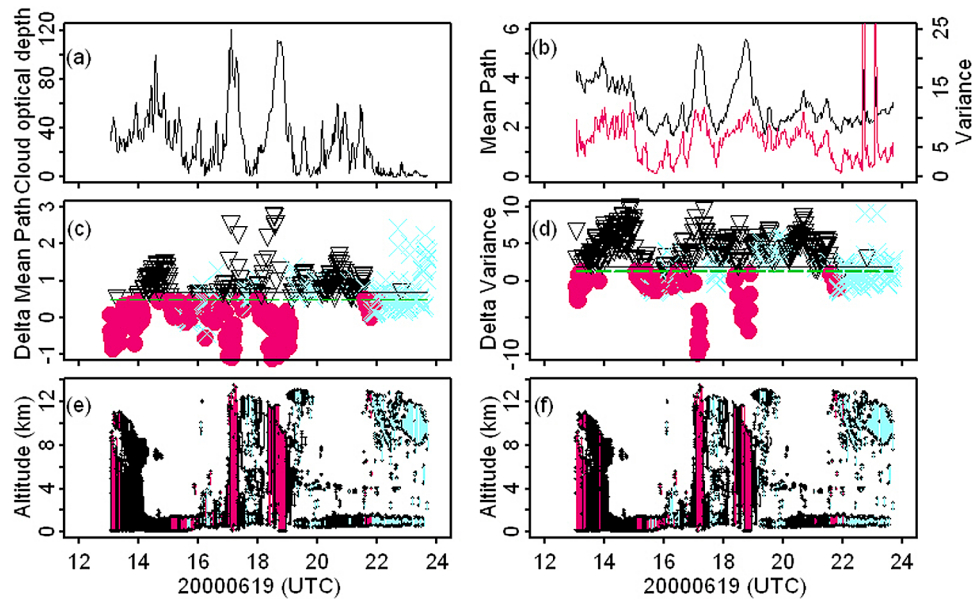


Figure 8. The same as Figure 5, but for 19 June 2000.

3.4. Case 4 (19 June 2000)

[20] The case of 19 June 2000, shown in Figure 8, is another interesting case. The clouds between 13.1 UTC and 14.3 UTC were deep convective clouds with a broken layer in the early morning. Those deep convective clouds occurred again at 17.5 UTC and late around 18.7 UTC. For the rest of the time, a low-level cloud persisted with occasionally scattered upper-level clouds. As shown in Figures 8c and 8d, under physically thick cloud conditions, the Δ -variance is more sensitive to diagnose multilayer clouds than the Δ -mean, which further corroborates the finding in case 2. The cloud field classification from the photon path length method is very consistent with the MMCR-MPL observation except for a few periods.

[21] Within the period of 14.3–15.1 UTC, both Δ -mean and Δ -variance diagnosed the clouds as being multilayered, whereas the MMCR-MPL detected only two scattered upper-level clouds around 14.6 UTC and 14.7 UTC. It could be either the 3-D effect of scattered upper-level clouds impacted the nearby radiation field or some other clouds existed but were not detected by the MMCR-MPL. A similar situation occurred for the period of 20.0–21.7 UTC. More interestingly, for the period of 15.1–15.6 UTC, both photon path length method and the MMCR-MPL detected a single-layer cloud, except for the period between 15.4 and 15.5 UTC. During this 6 min interval, both Δ -mean and

Δ -variance diagnosed the clouds as multilayer clouds. It could be the situation that a cloud was aloft somewhere but beyond the field of view (FOV) of the MMCR-MPL.

4. Aggregate Statistics and Sensitivity Study

[22] The case studies provide some insights on how the photon path length method works for diagnosing multilayer clouds. It is important to assess possible “missed” clouds by the MMCR-MPL statistically. We applied this method to 1 year (year 2000) measurements at the ARM SGP site. Over 59% of all clouds (daytime and nighttime) were detected by MMCR-MPL as single-layer clouds, whereas about 34% of all clouds occurred in the daytime with solar zenith angles less than 70° . Most clouds during the daytime were optically thin clouds, and only 32.2% of those single-layer clouds were optically thick ($\tau > 10$). About 56% of those optically thick clouds were detected by the MMCR-MPL as single-layer clouds.

[23] As listed in Table 1, with the normal threshold, the consistency rate between the photon path length method and the MMCR-MPL detection were 66.5% and 56.4% for single-layer clouds and multilayer clouds, respectively. It means that with the normal threshold the photon path length method diagnosed 43.6% of multilayer clouds as being single layered. In the meantime, about 33.5% of the MMCR-MPL detected single-layer clouds were diagnosed

Table 1. Aggregate Statistic Under the Normal Threshold for the Year 2000 at the ARM SGP Site^a

Normal Threshold	MMCR-MPL Single-Layer Cloud	MMCR-MPL Multilayer Cloud
A band single-layer cloud	66.5% (35.8%)	43.6% (20.1%)
A band multilayer cloud	33.5% (18.0%)	56.4% (26.1%)

^aThe values outside parentheses are the percentages of A band detection over analyzed MMCR-MPL detection (with solar zenith angle less than 70° and optical depth larger than 10), whereas the values in parentheses are the percentages of A band detection over all analyzed clouds.

Table 2. Same as Table 1 But Under the Conservative Threshold

Conservative Threshold	MMCR-MPL Single-Layer Cloud	MMCR-MPL Multilayer Cloud
A band single-layer cloud	72.3% (39.0%)	52.7% (24.3%)
A band multilayer cloud	27.7% (14.9%)	47.3% (21.8%)

by the photon path length method as multilayer clouds. It suggests that one third of the MMCR-MPL-detected optically thick single-layer clouds had been influenced radiatively by other “missed” clouds.

[24] Even with the conservative threshold (Table 2) that allowed over half of the MMCR-MPL detected multilayer clouds to be classified as single-layer clouds, there were still 27.7% of the MMCR-MPL detected single-layer clouds that were diagnosed by the photon path length method as multilayer clouds. With this conservative estimation, at least, one quarter of the MMCR-MPL-detected single-layer clouds had been influenced by other clouds; either the clouds were composed of small hydrometeors and/or thinner than the radar sample volume depth resulting in partial beam filling or somewhere beyond the FOV of the MMCR-MPL.

5. Conclusion

[25] From the perspective of the GCM, the most important reason to do radiative calculations in any form is to obtain the broadband heating rates. As the BBHRP products in the ARM program primarily use cloud products from the MMCR-MPL, “missed” cloud layers in current MMCR-MPL retrievals result in substantial errors in the BBHRP products. To flag those potential multilayer clouds “missed” by MMCR-MPL, we developed a detection method based on photon path length distribution. Our photon path length method is to estimate photon path length information from the low-level single-layer cloud structure that can be accurately observed by the MMCR-MPL and optical properties from the MFRSR and to detect the “missed” clouds. As multiple scattering within the cloud layers and between layers would substantially enhance the photon path length, the multilayer clouds can be diagnosed by evaluating the estimated photon path information against observed photon path length information from a co-located RSS. Using a Monte Carlo radiative transfer model, we parameterized both mean and variance of the photon path length distribution for single-layer cloud structure, based on the classic diffusion theory. The maximum errors between the simulated and fitted mean and variance were 0.5 and 1.3, respectively. Those maximum fitting errors provide a measure of detection uncertainty in both Δ -mean and Δ -variance schemes.

[26] We processed the measurements of MMCR-MPL, RSS, and MFRSR at the ARM SGP site for the year 2000. Cases studies illustrated the consistency between MMCR-MPL detection and the photon path length method under most conditions. Also for the thick, low-level clouds, Δ -variance is more sensitive to diagnose the multilayer clouds than Δ -mean. Even with both normal and conservative thresholds that allow some multilayer clouds to be diagnosed as single-layer clouds, the photon path length method detected some multilayer clouds that were detected by the MMCR-MPL as single-layer clouds. It means that the upper

layer clouds “missed” by the MMCR-MPL had significant effects on radiation, e.g., photon path length. On the basis of 1 year statistics at the ARM SGP site, we found that about 27.7% of single-layer clouds detected by the MMCR-MPL with solar zenith angle less than 70° and optical depth greater than 10 could be multilayer clouds. It is a conservative estimation with the conservative threshold that treats over half of the MMCR-MPL detected multilayer clouds to be classified as single-layer clouds.

[27] Our photon path length method has some limitations. It is based on a passive instrument, which is only applicable during daytime. Also, our parameterization of both mean and variance is based on diffusion theory with optically thick assumption. Nonetheless, within the detection limits, the photon path length method diagnosed over 27% of the MMCR-MPL detected single-layer clouds could be influenced radiatively by other “missed” clouds. We should flag those periods and be cautious of any radiation application of the MMCR-MPL measurements during those periods. Furthermore, under other conditions, optically thin clouds or clouds that occurred during nighttime, we suspect that a substantial portion of single-layer clouds detected by the MMCR-MPL could also be influenced by some “missed” clouds or by the 3-D effects of clouds. Without accurately detecting those “missed” clouds, the BBHRP will be inaccurate. Our results echo the need for a true 3-D scanning radar for radiation applications. Also, our photon path length information is retrieved from the modest resolution measurements of RSS. Only the first two moments (mean and variance) of photon path length distribution can be inferred, which further limits our detection capability of 3-D cloud effects. With a high-resolution oxygen A band spectrometer [Min et al., 2004], we expect a more powerful diagnosis for 3-D cloud effects from retrieved higher moments of photon path length distribution.

[28] **Acknowledgments.** This research was supported by the Office of Science (BER), U.S. Department of Energy through the Atmospheric Radiation Measurement (ARM) Grant DE-FG02-03ER63531, and by the NOAA Educational Partnership Program with Minority Serving Institutions (EPP/MSI) under Cooperative Agreements NA17AE1625 and NA17AE1623.

References

- Clothiaux, E. E., T. P. Ackerman, G. G. Mace, K. P. Moran, R. T. Marchand, M. A. Miller, and B. E. Martner (2000), Objective determination of cloud heights and radar reflectivities using a combination of active remote sensors at the ARM CART sites, *J. Appl. Meteorol.*, *39*, 645.
- Davis, A. B., and A. Marshak (2002), Space-time characteristics of light transmitted through dense clouds: A Green’s function analysis, *J. Atmos. Sci.*, *59*, 2713–2727.
- Fischer, J., and H. Grassl (1991), Detection of cloud-top height from backscattered radiances within the oxygen A band, Part 1: Theoretical study, *J. Appl. Meteorol.*, *30*, 1245.
- Fischer, J., W. Cordes, A. Schmitz-Peiffer, W. Renger, and P. Morel (1991), Detection of cloud-top height from backscattered radiances

- within the oxygen A band, part 2: Measurements, *J. Appl. Meteorol.*, *30*, 1260.
- Grechko, Y. I., V. I. Dianov-Klokov, and I. P. Malkov (1973), Aircraft measurements of photon paths in reflection and transmission of light by clouds in the 0.76 μm oxygen band, *Atmos. Ocean Phys.*, *9*, 262.
- Harrison, L., and Q.-L. Min (1997), Photon path length distributions in cloudy atmospheres from ground-based high-resolution O₂ A band spectroscopy, in *IRS'96: Current Problems in Atmospheric Radiation*, edited by W. L. Smith and K. Stamnes, p. 594, A. Deepak, Hampton, Va.
- Irvine, W. M. (1964), The formation of absorption bands and the distribution of photon optical paths in a scattering atmosphere, *Bull. Astron. Inst. Neth.*, *17*, 266–279.
- Irvine, W. M. (1966), The shadowing effect in diffuse, *J. Geophys. Res.*, *71*(12), 2931–2937, doi:10.1029/JZ071i012p02931.
- Min, Q.-L., and L. C. Harrison (1996), Cloud properties derived from surface MFRSR measurements and comparison with GOES results at the ARM SGP site, *Geophys. Res. Lett.*, *23*(13), 1641, doi:10.1029/96GL01488.
- Min, Q.-L., and L. C. Harrison (1999), Joint statistics of photon path length and cloud optical depth, *Geophys. Res. Lett.*, *26*(10), 1425, doi:10.1029/1999GL900246.
- Min, Q.-L., and E. E. Clothiaux (2003), Photon path length distributions inferred from rotating shadowband spectrometer measurements at the atmospheric Radiation Measurements Program Southern Great Plains site, *J. Geophys. Res.*, *108*(D15), 4465, doi:10.1029/2002JD002963.
- Min, Q.-L., and L. C. Harrison (2004), Retrieval of atmospheric optical depth profiles from downward-looking high-resolution O₂ A band measurements: Optically thin conditions, *J. Atmos. Sci.*, *61*, 2469–2477.
- Min, Q.-L., L. C. Harrison, and E. E. Clothiaux (2001), Joint statistics of photon path length and cloud optical depth: Case studies, *J. Geophys. Res.*, *106*(D7), 7375, doi:10.1029/2000JD900490.
- Min, Q.-L., L. C. Harrison, P. Kiedron, J. Berndt, and E. Joseph (2004), A high-resolution oxygen A band and water vapor band spectrometer, *J. Geophys. Res.*, *109*, D02202, doi:10.1029/2003JD003540.
- O'Brian, D. M., and R. M. Mitchell (1992), Error estimates for retrieval of cloud top pressure using absorption in the A band of oxygen, *J. Appl. Meteorol.*, *31*, 1179.
- Pfeilsticker, K., F. Erle, H. Veitel, and U. Platt (1998), First geometrical path lengths probability density function derivation of the skylight from spectroscopically highly resolving oxygen A band observations, 1: Measurement technique, atmospheric observations and model calculations, *J. Geophys. Res.*, *103*(D10), 11,483–11,504, doi:10.1029/98JD00725.
- Portmann, R. W., S. Solomon, R. W. Sanders, and J. S. Danel (2001), Cloud modulation of zenith sky oxygen path lengths over Voulder, Colorado: Measurements versus model, *J. Geophys. Res.*, *106*(D1), 1139, doi:10.1029/2000JD900523.
- Van de Hulst, H. C. (1980), *Multiple Light Scattering, Tables, Formulas and Applications*, vol. 1 and 2, Academic, London.
- Veitel, H., O. Funk, C. Kruz, U. Platt, and K. Pfeilsticker (1998), Geometrical path length probability density functions of the skylight transmitted by midlatitude cloudy skies: Some case studies, *Geophys. Res. Lett.*, *25*(17), 3355, doi:10.1029/98GL02506.

S. Li and Q. Min, Atmospheric Sciences Research Center, State University of New York at Albany, Albany, NY 12203, USA. (min@asrc.cestm.albany.edu)